

ASAS-SN follow-up of IceCube high-energy neutrino alerts

Jannis Necker ^{1,2*}, Thomas de Jaeger ^{3†}, Robert Stein ^{1,2,4}, Anna Franckowiak ^{1,5}, Benjamin J. Shappée ³, Marek Kowalski ^{1,2}, Christopher S. Kochanek^{6,7}, Krzysztof Z. Stanek^{6,7}, John F. Beacom ^{8,6,7}, Dhvanil D. Desai ³, Kyle Neumann ⁶, Tharindu Jayasinghe ⁶, T. W.-S. Holoién ^{9‡}, Todd A. Thompson^{6,7}, Simon Holmbo ¹⁰

¹Deutsches Elektronen Synchrotron DESY, Platanenallee 6, 15738 Zeuthen, Germany

²Institut für Physik, Humboldt-Universität zu Berlin, D-12489 Berlin, Germany

³Institute for Astronomy, University of Hawaii, 2680 Woodlawn Drive, Honolulu, HI 96822, USA.

⁴Division of Physics, Mathematics, and Astronomy, California Institute of Technology, Pasadena, CA 91125, USA

⁵Fakultät für Physik & Astronomie, Ruhr-Universität Bochum, D-44780 Bochum, Germany

⁶Department of Astronomy, The Ohio State University, 140 W. 18th Avenue, Columbus, OH 43210, USA

⁷Center for Cosmology and AstroParticle Physics (CCAPP), The Ohio State University, 191 W. Woodruff Avenue, Columbus, OH 43210, USA.

⁸Department of Physics, The Ohio State University, 191 W. Woodruff Ave., Columbus, OH 43210, USA.

⁹The Observatories of the Carnegie Institution for Science, 813 Santa Barbara St., Pasadena, CA 91101, USA.

¹⁰Department of Physics and Astronomy, Aarhus University, Ny Munkegade 120, DK-8000 Aarhus C, Denmark.

Accepted XXX. Received YYY; in original form ZZZ

ABSTRACT

We report on the search for optical counterparts to IceCube neutrino alerts released between April 2016 and August 2021 with the All-Sky Automated Survey for SuperNovae (ASAS-SN). Despite the discovery of a diffuse astrophysical high-energy neutrino flux in 2013, the source of those neutrinos remains largely unknown. Since 2016, IceCube has published likely-astrophysical neutrinos as public realtime alerts. Through a combination of normal survey and triggered target-of-opportunity observations, ASAS-SN obtained images within 1 hour of the neutrino detection for 20% (11) of all observable IceCube alerts and within one day for another 57% (32). For all observable alerts, we obtained images within at least two weeks from the neutrino alert. ASAS-SN provides the only optical follow-up for about 17% of IceCube’s neutrino alerts. We recover the two previously claimed counterparts to neutrino alerts, the flaring-blazar TXS 0506+056 and the tidal disruption event AT2019dsg. We investigate the light curves of previously-detected transients in the alert footprints, but do not identify any further candidate neutrino sources. We also analysed the optical light curves of Fermi 4FGL sources coincident with high-energy neutrino alerts, but do not identify any contemporaneous flaring activity. Finally, we derive constraints on the luminosity functions of neutrino sources for a range of assumed evolution models.

Key words: neutrinos – supernovae: general – gamma-ray burst: general

1 INTRODUCTION

Neutrinos are unique messengers from the high-energy Universe. Produced through interactions of high-energy cosmic rays with ambient matter and photon fields, they provide an unambiguous tracer of the sites of hadronic acceleration (see Ahlers & Halzen 2018 for a recent review). Following the discovery of a diffuse astrophysical neutrino flux by the IceCube collaboration (Aartsen et al. 2015; Aartsen et al. 2014) there is now a major effort to identify their origin. No significant clustering has yet been found within the neutrino data alone, but a search for neutrino clusters from known gamma-

ray emitters found evidence for a correlation with the nearby Seyfert galaxy NGC 1068 at the 2.9σ level (Aartsen et al. 2020).

A complementary approach is to search directly for electromagnetic counterparts to individual high-energy neutrinos that have a high probability to be of astrophysical origin. Since 2016, the IceCube realtime program (Aartsen et al. 2017b) has published their detections of such events through public realtime alerts and two candidate electromagnetic counterparts have since been identified at the $\sim 3\sigma$ level. In 2017, the gamma-ray blazar TXS 0506+056 was observed in spatial coincidence with a high-energy neutrino during a period of electromagnetic flaring (Aartsen et al. 2018). A search for neutrino clustering from the same source revealed an additional neutrino flare in 2014–15 (IceCube Collaboration et al. 2018), during a period without any significant electromagnetic flaring activity (Garrappa et al. 2019). Theoretical models have confirmed that conditions in the source are consistent with the detection of one neutrino

* E-mail: jannis.necker@desy.de

† E-mail: dejager@hawaii.edu

‡ NHFP Einstein Fellow

after accounting for Eddington bias (Strotjohann et al. 2019). However, explaining the ‘‘orphan’’ neutrino flare in 2014/15 proved to be difficult (Reimer et al. 2019; Rodrigues et al. 2019). Statistically, the γ -ray blazar population contributes less than 27% to the diffuse neutrino flux (Aartsen et al. 2017c).

In 2019, the Tidal Disruption Event (TDE) AT2019dsg was associated with a high-energy neutrino (Stein et al. 2021b). Models have proposed various TDE neutrino production zones, including the wind, disk, or corona (see Hayasaki 2021 for a recent review) which are consistent with the detection of one high-energy neutrino. Radio observations of AT2019dsg confirm long-lived non-thermal emission from the source (Stein et al. 2021b; Cendes et al. 2021; Mohan et al. 2022; Matsumoto et al. 2022), but generally challenge models relying on the presence of an on-axis relativistic jet (Winter & Lunardini 2021). A population analysis constrained the contribution of TDEs to less than 39% of the diffuse neutrino flux (Stein 2019a). The coincidence of the TDE-like flare AT2019fdr with a high-energy neutrino (Reusch et al. 2021) strong dust echos in AT2019fdr and AT2019dsg motivated a search for similar events (van Velzen et al. 2021). A correlation at 3.7σ level of such flares with high-energy neutrino alerts was found. Taken together, these results suggest that the astrophysical neutrino flux has contributions from multiple source populations (Bartos et al. 2021). Other possible neutrino source populations include supernovae and gamma ray bursts.

Here we present the optical follow-up of 56 IceCube realtime alerts released between April 2016 and August 2021 with the All-Sky Automated Survey for SuperNovae (ASAS-SN; Shappee et al. 2014; Kochanek et al. 2017). ASAS-SN is a network of optical telescopes located around the globe that observes the visible sky daily. Its large field of view makes it well-suited for fast follow-up of IceCube alerts and enables searches for transient neutrino counterparts. In Section 2 we introduce the IceCube alert selection followed by the description of our optical follow-up. We present our analysis of possible counterparts in Section 3. We derive limits on neutrino source luminosity functions in Section 4 and discuss our conclusions in Section 5.

2 ICECUBE REALTIME ALERTS

The IceCube neutrino observatory, located at the South Pole, is the world’s largest neutrino telescope with an instrumented volume of one cubic kilometre (Aartsen et al. 2017a). The IceCube realtime program (Aartsen et al. 2017b) has released alerts since 2016 for individual high-energy (>100 TeV) neutrino events with a high probability to be of astrophysical origin. Initially, there were two alert streams: the *Extremely-High Energy* (EHE) alerts and the *High-Energy-Starting Events* (HESE) alerts. EHE events were reported with an estimate of the probability for the event to have an astrophysical origin, called *signalness*. This quantity was not reported for the HESE alerts. The first alert was issued on 27th April 2016 (Blaufuss 2016a). To increase the alert rate and to reduce the retraction rate, these streams were replaced with a unified ‘Astrotrack’ alert stream in 2019 (Blaufuss et al. 2019). All alerts are now assigned a signalness value, with the stream subdivided into Gold alerts (with a mean signalness of 50%) and Bronze alerts (mean signalness of 30%).

A total of 85 alerts were issued before September 2021. Twelve were later retracted because they were consistent with atmospheric neutrino background events. For two alerts, IC190504A and IC200227A, IceCube was not able to estimate the uncertainty of the spatial localisation. Since the coverage of these alerts cannot be calculated, we exclude these two alerts from the subsequent analysis. The remaining 71 neutrino alerts were candidates for our follow-up

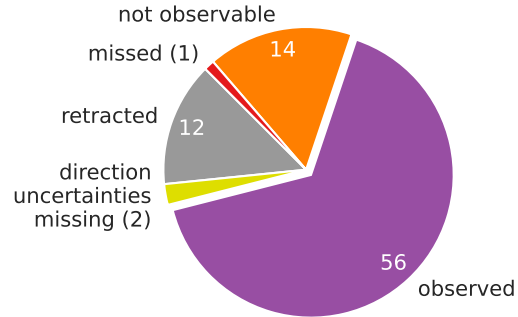


Figure 1. Statistics of ASAS-SN follow-up observations of the 85 IceCube alerts issued through to August 2021.

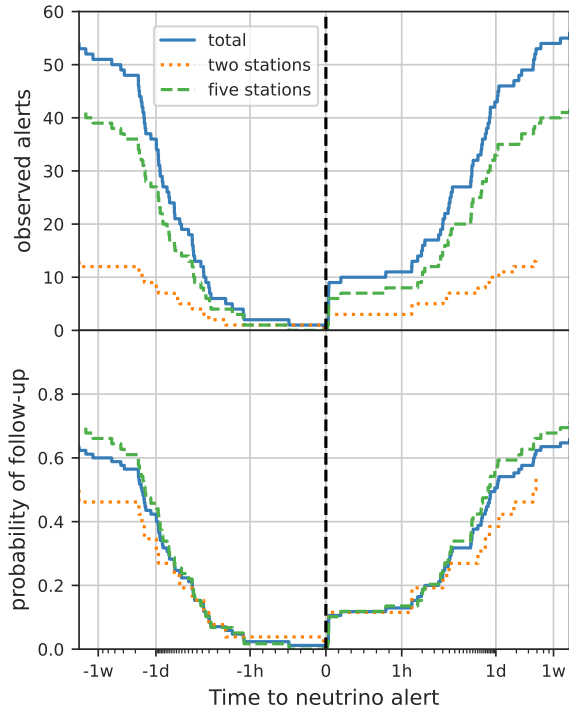


Figure 2. *Top panel:* Number of events triggered by ASAS-SN within about two weeks of the IceCube alert. In less than one day, 43 events have been observed over a total of 56 triggered by ASAS-SN between 2016–2021. *Bottom panel:* The mean probability of ASAS-SN observations for an IceCube alert. The boundary between the two station and the fully commissioned five station configuration is mid-2019.

program. A summary of the follow-up status of the alerts is shown in Figure 1. All IceCube neutrino alerts that could be followed up with ASAS-SN are listed in Table 1. The ones that could not be observed are listed in Table 2.

3 OPTICAL FOLLOW-UP WITH ASAS-SN

3.1 The All-Sky Automated Survey for Supernovae

ASAS-SN is ideal to search for optical counterparts to external triggers such as IceCube neutrino alerts or gravitational-wave events,

Event	R.A. (J2000) [deg]	Dec (J2000) [deg]	90% area [sq. deg.]	1d coverage [%]	14d coverage [%]	Signalness [%]	Refs
IC160427A	240.57	+9.34	1.4	100.0	100.0	-	Blaufuss (2016a)
IC160731A	214.50	-0.33	2.2	36.2	100.0	85	-
IC160814A	200.30	-32.40	12.0	0.0	100.0	-	Cowen (2016a)
IC161103A	40.83	+12.56	3.1	79.9	100.0	-	Taboada (2016)
IC161210A	46.58	+14.98	1.7	0.0	100.0	49	Blaufuss (2016b)
IC170312A	305.15	-26.61	0.9	0.0	100.0	-	Blaufuss (2017a)
IC170321A	98.30	-15.02	5.6	4.5	100.0	28	Blaufuss (2017b)
IC170922A	77.43	+5.72	1.3	100.0	100.0	57	Kopper & Blaufuss (2017)
IC171106A	340.00	+7.40	0.7	100.0	100.0	75	Taboada (2017)
IC181023A	270.18	-8.57	9.3	70.5	100.0	28	Blaufuss (2018b)
IC190104A	357.98	-26.65	18.5	14.0	100.0	-	Kopper (2019a)
IC190221A	268.81	-17.04	5.2	78.6	100.0	-	Taboada (2019)
IC190331A	337.68	-20.70	0.4	0.0	100.0	-	Kopper (2019b)
IC190503A	120.28	+6.35	1.9	100.0	100.0	36	Blaufuss (2019b)
IC190619A	343.26	+10.73	27.2	100.0	100.0	55	Blaufuss (2019c)
IC190629A	27.22	+84.33	5.0	0.0	70.6	34	Blaufuss (2019d)
IC190704A	161.85	+27.11	21.0	100.0	100.0	49	Santander (2019a)
IC190712A	76.46	+13.06	92.0	0.0	13.1	30	Blaufuss (2019e)
IC190730A	225.79	+10.47	5.4	100.0	100.0	67	Stein (2019b)
IC190922B	5.76	-1.57	4.5	100.0	100.0	51	Blaufuss (2019f)
IC191001A	314.08	+12.94	25.5	100.0	100.0	59	Stein (2019d)
IC191122A	27.25	-0.04	12.2	100.0	100.0	33	Blaufuss (2019h)
IC191204A	79.72	+2.80	11.6	98.8	100.0	33	Stein (2019e)
IC191215A	285.87	+58.92	12.8	0.0	12.4	47	Stein (2019f)
IC191231A	46.36	+20.42	35.6	100.0	100.0	46	Santander (2019c)
IC200107A	148.18	+35.46	7.6	0.0	78.2	50*	Stein (2020a)
IC200109A	164.49	+11.87	22.5	77.7	100.0	77	Stein (2020b)
IC200117A	116.24	+29.14	2.9	0.0	100.0	38	Lagunas Gualda (2020a)
IC200410A	242.58	+11.61	377.9	38.0	100.0	31	Stein (2020c)
IC200425A	100.10	+53.57	18.8	7.2	100.0	48	Santander (2020a)
IC200512A	295.18	+15.79	9.8	62.5	100.0	32	Lagunas Gualda (2020b)
IC200523A	338.64	+1.75	90.6	24.5	100.0	25	Blaufuss (2020b)
IC200530A	255.37	+26.61	25.3	92.4	100.0	59	Stein (2020d)
IC200614A	33.84	+31.61	47.8	35.2	100.0	42	Blaufuss (2020c)
IC200615A	142.95	+3.66	5.9	97.9	100.0	83	Lagunas Gualda (2020c)
IC200620A	162.11	+11.95	1.7	100.0	100.0	32	Santander (2020b)
IC200911A	51.11	+38.11	52.7	46.5	100.0	41	Lagunas Gualda (2020d)
IC200916A	109.78	+14.36	4.2	100.0	100.0	32	Blaufuss (2020d)
IC200926A	96.46	-4.33	1.7	100.0	100.0	44	Lagunas Gualda (2020f)
IC200929A	29.53	+3.47	1.1	65.1	100.0	47	Lagunas Gualda (2020g)
IC201007A	265.17	+5.34	0.6	0.0	100.0	88	Santander (2020c)
IC201021A	260.82	+14.55	6.9	2.6	100.0	30	Lagunas Gualda (2020h)
IC201114A	105.25	+6.05	4.5	100.0	100.0	56	Blaufuss (2020g)
IC201115A	195.12	+1.38	6.6	0.0	100.0	46	Lagunas Gualda (2020i)
IC201120A	307.53	+40.77	64.3	82.5	100.0	50	Lagunas Gualda (2020j)
IC201130A	30.54	-12.10	5.4	100.0	100.0	15	Lagunas Gualda (2020k)
IC201209A	6.86	-9.25	4.7	100.0	100.0	19	Lagunas Gualda (2020l)
IC201221A	261.69	+41.81	8.9	0.0	100.0	56	Blaufuss (2020h)
IC201222A	206.37	+13.44	1.5	100.0	100.0	53	Blaufuss (2020i)
IC210210A	206.06	+4.78	2.8	100.0	100.0	65	Lagunas Gualda (2021a)
IC210503A	143.53	+41.81	102.6	27.1	100.0	41	Santander (2021a)
IC210510A	268.42	+3.81	4.0	0.0	100.0	28	Santander (2021b)
IC210608A	337.41	+18.37	109.7	94.8	100.0	31	Lagunas Gualda (2021b)
IC210629A	340.75	+12.94	6.0	100.0	100.0	35	Santander (2021d)
IC210717A	46.49	-1.34	30.0	69.2	100.0	50*	Lagunas Gualda (2021c)
IC210811A	270.79	+25.28	3.2	100.0	100.0	66	Santander (2021f)

*For offline selected events no, signalness is given. Because they are promising events that were selected by hand, we assume a signalness of 50%

Table 1. A summary of the 56 neutrino alerts followed up by ASAS-SN. In the first three column we list the name of the alert and its position. In columns three to six we give the 90% rectangular localisation of the neutrino as sent out in the GCN and the fraction of this area covered by ASAS-SN in the first 24 hours and 14 days, respectively, after the neutrino arrival. Finally, we list the signalness of the event and the reference to the original IceCube GCN. For HESE events no signalness was given and we neglect these events to be conservative.

Event	R.A. (J2000) [deg]	Dec (J2000) [deg]	90% area [sq. deg.]	Reason	Refs
IC160806A	122.81	-0.81	0.0	proximity to sun	Cowen (2016b)
IC171015A	162.86	-15.44	14.9	proximity to sun	Blaufuss (2017c)
IC180908A	144.58	-2.13	6.3	proximity to sun	Blaufuss (2018a)
IC181014A	225.15	-34.80	10.5	proximity to sun	Taboada (2018)
IC190124A	307.4	-32.18	2.0	proximity to sun	Blaufuss (2019a)
IC190819A	148.8	+1.38	9.3	proximity to sun	Santander (2019b)
IC190922A	167.43	-22.39	32.2	proximity to sun	Stein (2019c)
IC191119A	230.1	+3.17	61.2	proximity to sun	Blaufuss (2019g)
IC200421A	87.93	+8.23	24.4	operation	Blaufuss (2020a)
IC200806A	157.25	+47.75	1.8	proximity to sun	Stein (2020e)
IC200921A	195.29	+26.24	12.0	proximity to sun	Lagunas Gualda (2020e)
IC200926B	184.75	+32.93	9.0	proximity to sun	Blaufuss (2020e)
IC201014A	221.22	+14.44	1.9	proximity to sun	Blaufuss (2020f)
IC210516A	91.76	+9.52	2.2	proximity to sun	Santander (2021c)
IC210730A	105.73	+14.79	6.6	proximity to sun	Santander (2021e)

Table 2. A summary of the 15 neutrino alerts that could not be observed by ASAS-SN. We list the event name and position in the first three columns. The area of the 90% rectangular localisation of the neutrino is listed in column four and the reference to the IceCube GCN in column 5.

because it is the only ground-based survey to map the visible sky daily to a depth of $g = 18.5$ mag (Shappee et al. 2014; Kochanek et al. 2017). ASAS-SN started late 2013 with its first unit, Brutus, located on Haleakala in Hawaii (USA). Shortly after, in 2014, ASAS-SN expanded with a second unit, Cassius, situated at Cerro Tololo International Observatory (CTIO) in Chile. Since late-2017, ASAS-SN is composed of five stations located in both hemispheres: the two original stations (Cassius and Brutus), Paczynski, also situated at CTIO in Chile, Leavitt at McDonald Observatory in Texas (USA), and finally Payne-Gaposchkin at the South African Astrophysical Observatory (SAAO) in Sutherland, South Africa. The two original units used a V-band filter until late-2018. The new units were installed using g -band filters and the two old units were switched from V to g after roughly a year of V- and g -band overlap. Each unit consists of four 14-cm aperture Nikon telephoto lenses, each with a 4.47 by 4.47-degree field of view. They are hosted by Las Cumbres Observatory (Brown et al. 2013).

The ASAS-SN survey has two modes of operation (de Jaeger et al. 2022): a normal survey operation mode and a Target-of-Opportunity mode (ToO) to get rapid imaging follow-up of multi-messenger alerts. During normal operations, each ASAS-SN field is observed with three dithered 90-second exposures with ~ 15 seconds of overheads between each image, for a total of ~ 315 seconds per field. For the ToO mode, we trigger immediately if there is a site that can observe the IceCube neutrino region. Thanks to the four sites, this is often the case. We obtain $\sim 15 - 20$ exposures for the pointing closest to the centre of the search region to go deeper and discover fainter candidates. All the images obtained from the ToO or the normal survey are processed and analysed in realtime by the standard ASAS-SN pipeline. A full description of the ASAS-SN optical counterpart search strategy can be found in de Jaeger et al. (2022).

Prior to May 2017, only normal operation images were available. Once the ToO mode was implemented, we triggered on all the IceCube neutrino alerts and obtained images as soon as possible, in some cases within three minutes of the alert arrival time (IC190221A, IC190503A, IC200911A, IC201114A, IC201130A, IC210210A, and IC210811A). For one event (IC161103A), ASAS-SN was observing the respective localisation region as part of normal survey operations at the time of the neutrino arrival, resulting in images taken

105 seconds before and 2.5 sec after the alert arrival time. Since late 2017, there generally is a normal operations image (~ 18.5 mag) taken within a day if there are no weather or technical issues and the search region is not Sun or Moon constrained. The bottom panel of Figure 2 shows the cumulative distributions of observed events per year.

To estimate the completeness of our observations, we draw lightcurves on random locations all over the sky. We inject simulated SN Ia lightcurves and test whether ASAS-SN would have detected the simulated supernova. For each lightcurve this is repeated 100 times. This gives a completeness down to 16.5 mag in V-Band and 17.5 mag in g -band, respectively. The analysis will be described in Desai et al. (2022, in prep.).

Fourteen neutrino alerts had a localisation too close to the Sun to be observed and one alert was missed due to the short observing window (less than 2 hours), leaving 56 that were followed up out of 71 real IceCube alerts. The top panel in Figure 2 shows the cumulative number of events observed by ASAS-SN within about two weeks from the neutrino arrival, where the right side shows events observed after the neutrino arrival. Thanks to our strategy, we managed to observe 11 of the 56 triggered alerts in less than 1 hour (20%) among which nine were observed in less than five minutes, another four in less than two hours (7%), and 28 in less than one day (50%). This illustrates our ability to promptly observe the majority of the IceCube alerts independent of the time or localisation. Finally, another thirteen events were observed between 24 hours and two weeks (23%; see Figure 2): four within two days, two in less than three days, four within four days, one in less than five days, and two within two weeks. Note that the longest delays in observation (IC200107A and IC201221A) were due to observability constraints or bad weather. So within at most two weeks, we observed all of the neutrino alerts that have not been retracted (12), have a well defined search region, and satisfy our observational restrictions: (1) the Sun is at least 12 degrees below the horizon, (2) the airmass is at most two, (3) the Hour Angle is at most five hours, and (4) the minimum distance to the Moon is larger than 20° . The left side of the top panel in Figure 2 shows the cumulative number of events that were serendipitously observed during routine observations. For 36 events we obtained images within 24 hours before the alert, which allows us to put better constraints

on candidates. The localisation region of one alert (IC200530A) was observed about 30 minutes before the neutrino arrival and another one (IC161103A) was being observed at the time of neutrino arrival. We also show the distributions for the periods before and after mid-2019. This marks the commissioning of the full five stations and the switch of the first stations to g-band (two stations and five stations in Figure 2, respectively). We calculate the probability of any event being observed by dividing the number of followed-up events by the number of neutrino alerts. The results are shown in the bottom panel of Figure 2. For any given neutrino alert ASAS-SN has a probability of about 60% of obtaining observations. Most notably, the switch to the five station configuration significantly increased the probability of obtaining follow-up observations. For example it became 50% more likely to obtain observations within one day.

Finally, it is worth noting that for 12 out of the 71 alerts (around 17%) considered in this analysis, ASAS-SN observations are the only optical follow-up observation for the respective neutrino alert reported to the Gamma-ray Coordinates Network (GCN)¹.

3.2 Possible Counterpart Classes to High-Energy Neutrinos

The challenge in identifying counterparts to high-energy neutrino events is that there are many possible neutrino source populations, each with different electromagnetic properties. Again, ASAS-SN's large field of view, fast response time, and archival data for the whole sky make it well suited for discovering transient counterparts to the IceCube neutrino events. The list of promising candidate source classes include:

- **Supernovae with strong circumstellar material (CSM) interactions:** Models predict shock acceleration when the supernova ejecta interacts with the CSM (Murase et al. 2011; Murase 2018; Zirakashvili & Ptuskin 2016). For sufficiently high-density CSM, strong interactions produce the narrow emission lines defining a Type IIn supernova (Schlegel 1990; Chugai & Danziger 1994). The shock can produce high-energy neutrinos for several years but for typical Type IIn conditions the flux is expected to have dropped by an order of magnitude after the first year.
- **Gamma-ray bursts (GRBs) and supernovae with relativistic jets:** Particle acceleration can occur inside the jet or at the shock where the jet interacts with the star's envelope (Mészáros & Waxman 2001; Senno et al. 2016; Ando & Beacom 2005). This is true for both ‘successful’ jets which escape the star and ‘choked’ jets. In the first case the electromagnetic counterpart would be a stripped-envelope supernova with broad spectral features (a broad line Ic supernova, SN Ic-BL), and possibly a long GRB with an optical afterglow if the jet is aligned with the line of sight (Woosley & Bloom 2006). In the latter case the object would be a supernova Ic or Ib (Senno et al. 2016). In either case, a Type Ib/c SN with an explosion within a few days of the neutrino arrival is a compelling counterpart candidate, because the neutrino production is expected within tens of seconds of the core-collapse (Senno et al. 2016).
- **Tidal Disruption Events (TDEs):** TDEs have been proposed as high-energy neutrino sources, where neutrino production can occur in jets, outflows or winds, the accretion disk itself or the disk corona (see Hayasaki 2021 for a recent review). The TDE AT2019dsg was observed in coincidence with a high-energy neutrino alert, where the neutrino arrived 150 days after the optical peak of the TDE (Stein et al. 2021b). Another neutrino was observed about 300 days after

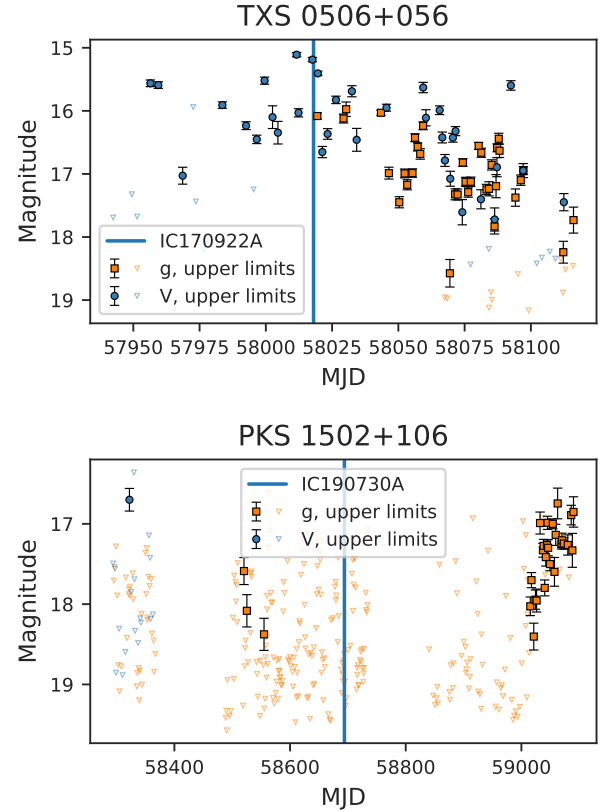


Figure 3. The ASAS-SN light curves of two blazars observed in spatial coincidence with high-energy neutrino alerts. We show 5σ detections and upper limits. The date of the corresponding neutrino arrival is marked with a vertical line.

the peak of the possible counterpart AT2019fdr (Reusch et al. 2021). The timescale for non-thermal emission in TDEs can span several hundred days, so any active TDE coincident with a high-energy neutrino is interesting. This is especially true in the light of recently found indication of correlation of high-energy neutrino alerts with TDE-like flares (van Velzen et al. 2021).

- **Active Galactic Nuclei (AGN) Flares:** AGN flares may produce high-energy neutrinos by accelerating particles in accretion shocks (Stecker et al. 1991). This is especially true for blazar flares, where a jet points towards the Earth (Petropoulou et al. 2015). The blazar TXS0506+056 was observed in coincidence with a high-energy neutrino alert while it was in a flaring state (Aartsen et al. 2018). Because these objects are numerous, we examined the ASAS-SN light curves of all Fermi 4FGL γ -ray detected blazars in the footprints of the neutrino alerts (see below and Figure 3).

3.3 Candidate Counterparts

Table 3 lists all transients identified by ASAS-SN in the 500 days prior to the neutrino arrival time excluding Type Ia SNe and dwarf novae (cataclysmic variables). The list includes the paring of the TDE AT2019dsg and IC191001 (Stein et al. 2021b). We do not detect the TDE AT2019fdr (Reusch et al. 2020) because it was too faint to trigger our transient detection pipeline.

The supernova SN 2019ah was spatially coincident with IC191119A. SN 2019ah was detected \sim 300 days before the neu-

¹ <https://gcn.gsfc.nasa.gov/selected.html>

Transient	ASAS-SN detection JD	IceCube alert	Alert epoch JD	$\Delta t = t_{\text{ASASSN}} - t_{\text{IceCube}}$ days	Transient type
ZTF18adicfwn (AT2020rng)	2459089.9	IC210608A	2459373.7	-284	Unknown
ATLAS19ljj (AT2019fxr)	2458634.9	IC200410A	2458950.5	-316	Unknown
ZTF19aapreis (AT2019dsg)	2458618.9	IC191001A	2458758.3	-139	TDE
ZTF19aadypig (SN 2019aah)	2458519.6	IC191119A	2458806.5	-287	SN II
ASASSN-18mx (SN 2018coq)	2458286.1	IC190619A	2458654.1	-368	SN II
ASASSN-17ot (AT2017hzv)	2458070.8	IC180908A	2458370.3	-300	Unknown

Table 3. An excerpt of Table B1 of the transients that occur at most 500 days before the corresponding neutrino was detected, excluding spectroscopically-confirmed type Ia supernovae and CVs where neutrino emission is not expected. We give the name of the Transient and the Julian Date of its discovery in the first two columns. Columns three and four list the corresponding IceCube alert and the neutrino arrival time. In the last two column we give the difference between transient discovery and neutrino arrival and the transient type.

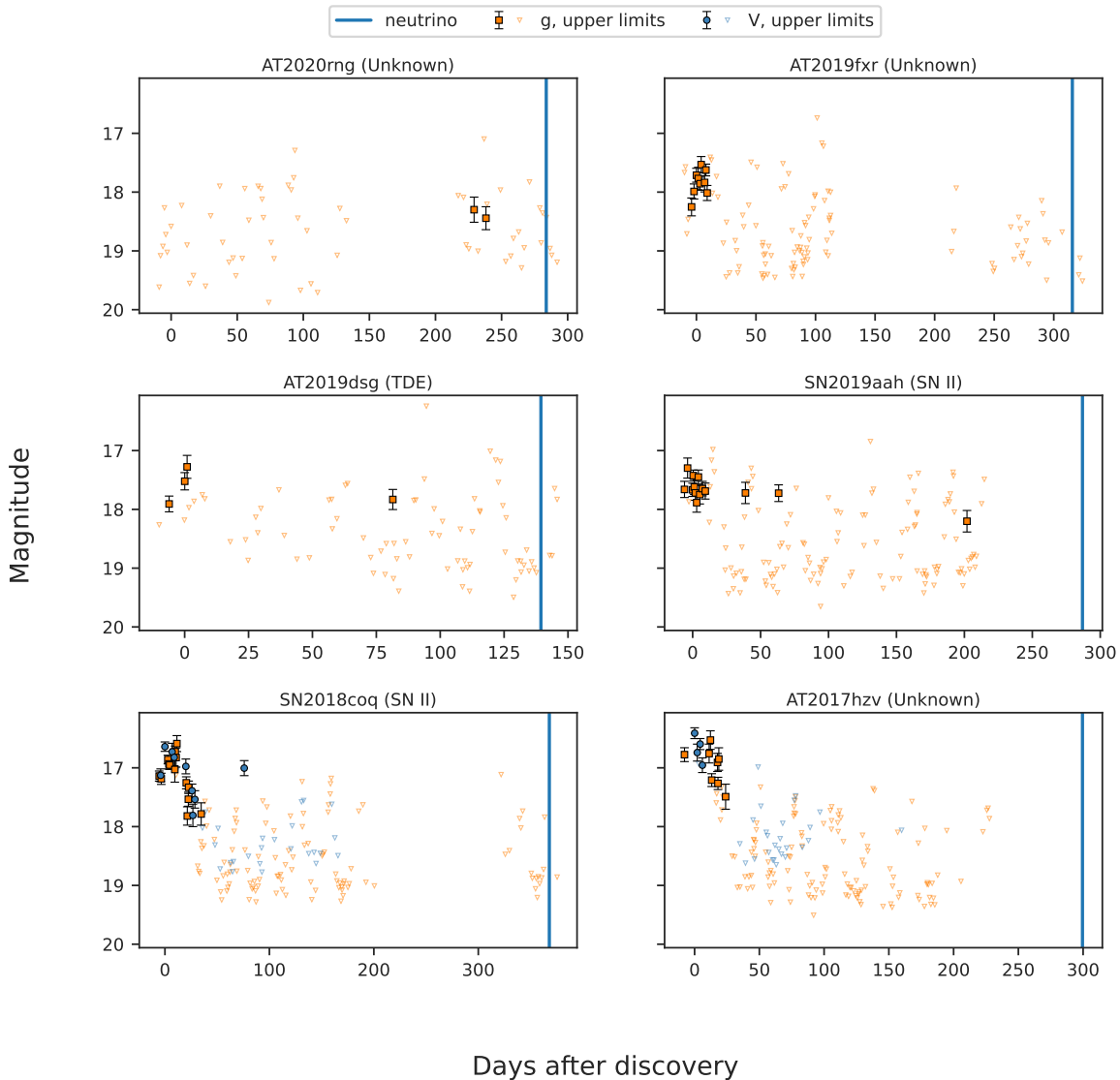


Figure 4. The ASAS-SN light curves for the transients found in the footprint of the IceCube neutrinos. We show 5σ detections and upper limits as a function of the days after the discovery dates listed in Table 3. For AT2020rng, we used the Zwicky Transient forced-photometry service facility and show the 5σ detections in the r- and g-band (see Fig. A). Vertical lines mark the time of the neutrino arrival.

trino alert (Nordin et al. 2019) and was classified 30 days after the discovery as a Type II supernovae (Dahiwale & Fremling 2020). Its spectrum does not show narrow emission lines, so there is no evidence for a strong CSM interaction to produce neutrino emission. The emission is predicted to be strongest near the optical peak (Murase et al. 2019; Zirakashvili & Ptuskin 2016), so we conclude that SN 2019aah is unrelated to the neutrino.

SN 2018coq was spatially coincident with IC190619A. It is also a Type II SN (Cartier 2018), discovered 370 days prior to the neutrino alert (Stanek 2018). Similar to SN 2019aah, its spectrum 13 days after the discovery does not show prominent narrow lines as a sign of CSM interaction. The supernova peaked even earlier relative to the neutrino than SN 2019aah, so SN 2018coq is unlikely related to IC190619A.

We find four neutrino-coincident events that could not be classified. All of them were first detected more than 280 days before the corresponding neutrino arrival. AT2017hzv (Brimacombe et al. 2017) and AT2019fxr (Tonry et al. 2019) faded on the time scale of a few weeks and are not detectable at the time of the neutrino arrival. The rapid fading suggest a supernova or AGN flare origin inconsistent with the neutrino arrival time which makes it unlikely they are associated with the corresponding neutrino.

For AT2020rng, we used the publicly available Zwicky Transient forced-photometry service (Masci et al. 2019). We only find sporadic detections surrounded by upper limits (see Figure A in the Appendix). This, together with the relatively bright host galaxy with a mean g-band magnitude of 15.3 mag suggests that AT2020rng is a subtraction artefact rather than a physical transient.

We also examined the ASAS-SN light curves of every Fermi 4FGL Blazar (Abdollahi et al. 2020; Ballet et al. 2020) within the footprint of a neutrino alert. We do not find any flaring activity coincident with the arrival of the corresponding neutrino, except for the previously-reported ASAS-SN observations of TXS 0506+056 (Aartsen et al. 2018). This light curve is shown in the top panel of Figure 3, with the source exhibiting an optical flare at the time of the neutrino detection.

The neutrino IC190730A was observed in spatial coincidence with the Flat Spectrum Radio Quasar (FSRQ) PKS 1502+106 (Stein 2019b; Franckowiak et al. 2020) and the ASAS-SN light curve for this object is shown in the lower panel of Figure 3. We confirm that the blazar was in a low optical state at the time of the neutrino arrival, as reported by Stein et al. (2019) and Steeghs et al. (2019). Time dependent radiation modeling found that the detection of a high-energy neutrino from this source is consistent with its multi-wavelength properties (Rodrigues et al. 2021).

4 LIMITS

While we do not find any new candidate counterpart transients in our follow-up campaign, we can use the non-detections to derive limits on neutrino source luminosity functions following the method of Stein et al. (2022, in prep.). Because we recover the two pre-existing source candidates (TXS 0506+056 and AT2019dsg), these non-detection limits do not apply to blazars or TDEs.

For an astrophysical neutrino with an electromagnetic counterpart, we can calculate the probability of detecting the counterpart based on the percentage of the neutrino localisation that was observed by ASAS-SN. For each neutrino this fraction is listed in Table 1 for one and fourteen days after the neutrino arrival. The probability of detecting a counterpart also depends on the probability for the neutrino to be of astrophysical origin. This is given by IceCube as the *signalness* (see Section 2 and Table 1). We will assume in the

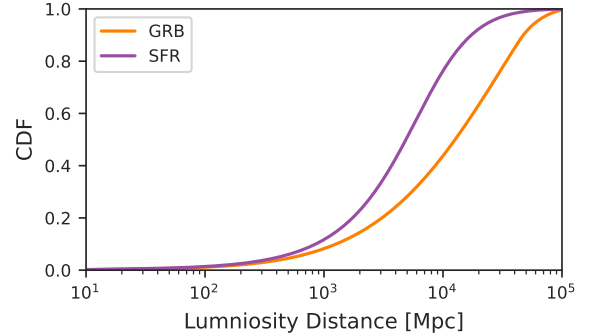


Figure 5. The relative cumulative neutrino flux at earth of neutrino source populations with a GRB-like and a SFR-like density evolution.

following that we would have observed a transient if it had reached 18.5 mag and adapt it as the limiting magnitude of our program.

At a 90% confidence level we can constrain the fraction of neutrino sources above our limiting magnitude to be no more than 39.3% and 15.3% for fast transients which reach their peak within two hours and one day, respectively. For transients that peak within fourteen days, the fraction is 10.3%. These constraints refer to the visibility of the transients and do not include any physical properties of the source classes.

To constrain physical populations of candidate neutrino sources we have to assume a rate $\dot{\rho}(z)$ at which the transients occur as a function of redshift z . We consider a GRB-like (Lien et al. 2014) and a star formation rate (SFR) like (Strolger et al. 2015) source evolution. Because the optical afterglow of a GRB rapidly fades on the timescale of a few days (Kann et al. 2010), we use the two hour coverage fraction of 15.3%. Interacting supernovae typically rise on a timescale of at least two weeks (Nyholm et al. 2020) so we use the 39.3% constraint for our coverage after 14 days. The cumulative neutrino fluxes at earth from these populations as calculated with `flarestack` (Stein et al. 2021a) are shown in Figure 5.

Assuming an absolute magnitude for the transient, we can compute the luminosity distance at which the transient would be at the apparent magnitude to which our follow-up program is complete. As a conservative choice we use the magnitude limit derived for the Type Ia SNe in ASAS-SN (see Section 3). Using the source evolutions from Figure 5, we derive the neutrino flux that would arise in this volume from the corresponding neutrino source population. Given our limits on the fraction of the population above our limiting magnitude we can convert this into constraints on the fraction of sources F_L above the source absolute magnitude as shown in Figure 6.

These results are not yet constraining for typical supernovae with absolute magnitudes up to around -21.5 . However, we can constrain the luminosity function of a neutrino source population with a GRB-like source evolution to produce counterparts that are below -27 magnitude in V-band about 54% of the cases and in g-band about 40% of the cases, one day after the neutrino arrival. This is the first such constraint on this timescale which is thanks to the high observation cadence and rapid follow-up of ASAS-SN.

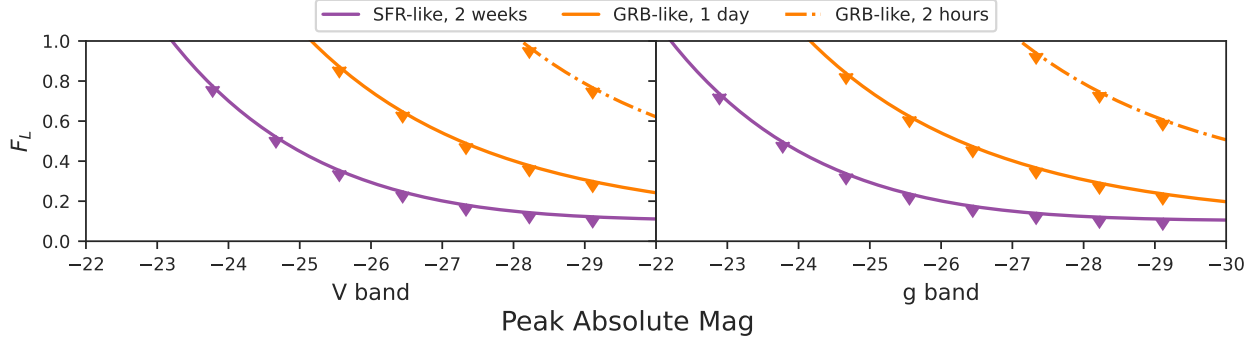


Figure 6. Constraints on the fraction F_L of a neutrino source population as a function of the intrinsic source Peak Absolute Magnitude.

5 CONCLUSIONS

We presented the ASAS-SN optical follow-up program for IceCube high-energy, astrophysical neutrino candidates. We observed the 90% localisation region of 56 alerts over the period from April 2016 until August 2021. Eleven of these alerts were covered within one hour after their detection. After 1 day we had observed 43 events and after two weeks we had observed the localisation regions for all 56 alerts to a limiting magnitude of ~ 18.5 . For 12 events (around 17%), this is the only optical follow-up. We did not detect any new coincident transients in our analysis, but we did recover the associations with the blazar TXS 05056+056 and the TDE AT2019dsg.

We find additional transients that we disfavour as counterparts of the corresponding neutrino. Given the non-detection of any transient counterpart in our search we derive upper limits on the luminosity function of different possible transient neutrino source populations.

Assuming the IceCube alert stream does not change, we can expect about 20 neutrino alerts per year. If our average coverage (18% after two hours and 94% after 14 days) does not change, we can set limits that are twice as strict on GRBs in 3.5 years and on CCSNe in 3 years, respectively.

The planned extension of IceCube, called IceCube-Gen2, is expected to increase the event rate significantly and improve the spatial resolution of through-going tracks (Aartsen et al. 2021). This will allow us to followup more neutrino alerts and cover a higher percentage of the smaller neutrino localisation area leading to an improved sensitivity to detect optical counterparts.

ACKNOWLEDGEMENTS

J.N. was supported by the Helmholtz Weizmann Research School on Multimessenger Astronomy, funded through the Initiative and Networking Fund of the Helmholtz Association, DESY, the Weizmann Institute, the Humboldt University of Berlin, and the University of Potsdam. Support for T.d.J. has been provided by NSF grants AST-1908952 and AST-1911074. R.S. and A.F. were supported by the Initiative and Networking Fund of the Helmholtz Association, Deutsches Elektronen Synchrotron (DESY). B.J.S. is supported by NSF grants AST-1907570, AST-1908952, AST-1920392, and AST-1911074. CSK and KZS are supported by NSF grants AST-1814440 and AST-1908570. J.F.B. is supported by National Science Foundation grant No. PHY-2012955. Support for TW-SH was provided by NASA through the NASA Hubble Fellowship grant HST-HF2-

51458.001-A awarded by the Space Telescope Science Institute, which is operated by the Association of Universities for Research in Astronomy, Inc., for NASA, under contract NAS5-265.

ASAS-SN is funded in part by the Gordon and Betty Moore Foundation through grants GBMF5490 and GBMF10501 to the Ohio State University, NSF grant AST-1908570, the Mt. Cuba Astronomical Foundation, the Center for Cosmology and AstroParticle Physics (CCAPP) at OSU, the Chinese Academy of Sciences South America Center for Astronomy (CAS-SACA), and the Villum Fonden (Denmark). Development of ASAS-SN has been supported by NSF grant AST-0908816, the Center for Cosmology and AstroParticle Physics at the Ohio State University, the Mt. Cuba Astronomical Foundation, and by George Skestos. Some of the results in this paper have been derived using the healpy and HEALPix packages.

The ZTF forced-photometry service was funded under the Heising-Simons Foundation grant #12540303 (PI: Graham).

DATA AVAILABILITY

All information about the IceCube neutrino alerts that we used are publicly available and can be accessed via the GCN archive for GOLD and BRONZE (https://gcn.gsfc.nasa.gov/amon_icecube_gold_bronze_events.html), the HESE (https://gcn.gsfc.nasa.gov/amon_hese_events.html) and EHE (https://gcn.gsfc.nasa.gov/amon_ehe_events.html) events. The ZTF forced-photometry service is publicly available (see <http://web.ipac.caltech.edu/staff/fmasci/ztf/forcedphot.pdf> for a description of the access).

REFERENCES

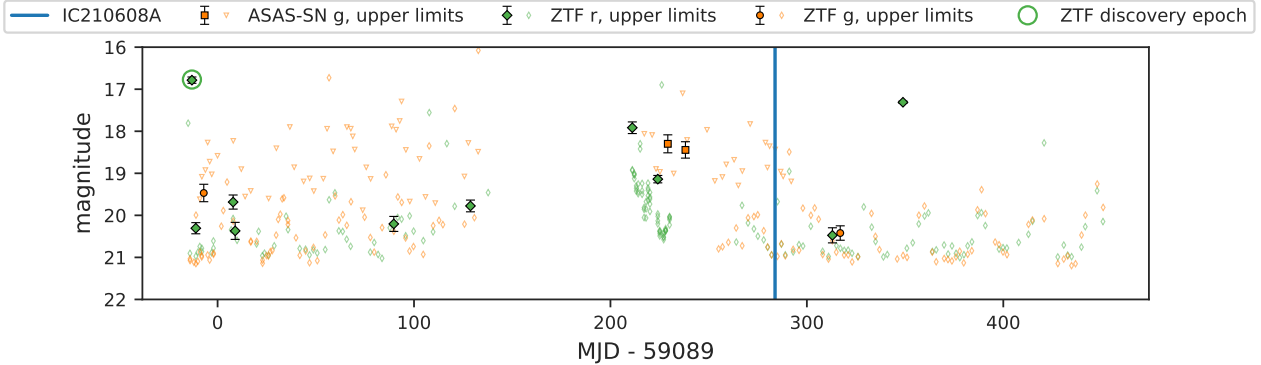
- Aartsen M. G., et al., 2014, *Phys. Rev. Lett.*, **113**, 101101
- Aartsen M. G., et al., 2015, *Phys. Rev. Lett.*, **115**, 081102
- Aartsen M. G., et al., 2017a, *JINST*, **12**, P03012
- Aartsen M. G., et al., 2017b, *Astroparticle Physics*, **92**, 30
- Aartsen M. G., et al., 2017c, *ApJ*, **835**, 45
- Aartsen M. G., et al., 2018, *Science*, **361**, eaat1378
- Aartsen M. G., et al., 2020, *Phys. Rev. Lett.*, **124**, 051103
- Aartsen M. G., et al., 2021, *Journal of Physics G Nuclear Physics*, **48**, 060501
- Abdollahi S., et al., 2020, *ApJS*, **247**, 33
- Ahlers M., Halzen F., 2018, *Progress in Particle and Nuclear Physics*, **102**, 73
- Ando S., Beacom J. F., 2005, *Phys. Rev. Lett.*, **95**, 061103

- Ballet J., Burnett T. H., Digel S. W., Lott B., 2020, arXiv e-prints, p. [arXiv:2005.11208](#)
- Bartos I., Veske D., Kowalski M., Marka Z., Marka S., 2021, *Astrophys. J.*, 921, 45
- Blaufuss E., 2016a, GCN Circular, [19363](#)
- Blaufuss E., 2016b, GCN Circular, [20247](#)
- Blaufuss E., 2017a, GCN Circular, [20857](#), 1
- Blaufuss E., 2017b, GCN Circular, [20929](#)
- Blaufuss E., 2017c, GCN Circular, [22016](#)
- Blaufuss E., 2018a, GCN Circular, 23214
- Blaufuss E., 2018b, GCN Circular, 23375
- Blaufuss E., 2019a, GCN Circular, 23785
- Blaufuss E., 2019b, GCN Circular, 24378
- Blaufuss E., 2019c, GCN Circular, 24854
- Blaufuss E., 2019d, GCN Circular, 24910
- Blaufuss E., 2019e, GCN Circular, 25057
- Blaufuss E., 2019f, GCN Circular, 25806
- Blaufuss E., 2019g, GCN Circular, 26258
- Blaufuss E., 2019h, GCN Circular, 26276
- Blaufuss E., 2020a, GCN Circular, 27612
- Blaufuss E., 2020b, GCN Circular, 27787
- Blaufuss E., 2020c, GCN Circular, 27941
- Blaufuss E., 2020d, GCN Circular, [28433](#)
- Blaufuss E., 2020e, GCN Circular, [28509](#)
- Blaufuss E., 2020f, GCN Circular, [28616](#)
- Blaufuss E., 2020g, GCN Circular, [28887](#)
- Blaufuss E., 2020h, GCN Circular, [29102](#)
- Blaufuss E., 2020i, GCN Circular, [29120](#)
- Blaufuss E., Kintscher T., Lu L., Tung C. F., 2019, in 36th International Cosmic Ray Conference (ICRC2019). p. 1021 ([arXiv:1908.04884](#))
- Brimacombe J., et al., 2017, The Astronomer's Telegram, [10967](#), 1
- Brown T. M., et al., 2013, *PASP*, **125**, 1031
- Cartier R., 2018, Transient Name Server Classification Report, [2018-927](#), 1
- Cendes Y., Alexander K. D., Berger E., Eftekhari T., Williams P. K. G., Chornock R., 2021, *Astrophys. J.*, 919, 127
- Chugai N. N., Danziger I. J., 1994, *MNRAS*, **268**, 173
- Cowen D. F., 2016a, GCN Circular, [19787](#), 1
- Cowen D., 2016b, GCN Circular, 19787, 1
- Dahiwale A., Fremling C., 2020, Transient Name Server Classification Report, [2020-601](#), 1
- Desai D., et al., 2022, The Volumetric Type Ia Supernovae Rate in ASAS-SN, in preparation
- Franckowiak A., et al., 2020, *ApJ*, **893**, 162
- Garrappa S., et al., 2019, *Astrophys. J.*, 880, 880:103
- Hayasaki K., 2021, *Nature Astronomy*, 5, 436
- IceCube Collaboration et al., 2018, *Science*, **361**, 147
- Kann D. A., et al., 2010, *Astrophys. J.*, 720, 1513
- Kochanek C. S., et al., 2017, *PASP*, **129**, 104502
- Kopper C., 2019a, GCN Circular, 23605
- Kopper C., 2019b, GCN Circular, [24028](#)
- Kopper C., Blaufuss E., 2017, GCN Circular, [21916](#)
- Lagunas Gualda C., 2020a, GCN Circular, 26802
- Lagunas Gualda C., 2020b, GCN Circular, 27719
- Lagunas Gualda C., 2020c, GCN Circular, 27950
- Lagunas Gualda C., 2020d, GCN Circular, [28411](#)
- Lagunas Gualda C., 2020e, GCN Circular, [28468](#)
- Lagunas Gualda C., 2020f, GCN Circular, [28504](#)
- Lagunas Gualda C., 2020g, GCN Circular, [28532](#)
- Lagunas Gualda C., 2020h, GCN Circular, [28715](#)
- Lagunas Gualda C., 2020i, GCN Circular, [28889](#)
- Lagunas Gualda C., 2020j, GCN Circular, [28927](#)
- Lagunas Gualda C., 2020k, GCN Circular, [28969](#)
- Lagunas Gualda C., 2020l, GCN Circular, [29012](#)
- Lagunas Gualda C., 2021a, GCN Circular, [29454](#)
- Lagunas Gualda C., 2021b, GCN Circular, [30153](#)
- Lagunas Gualda C., 2021c, GCN Circular, [30468](#), 1
- Lien A., Sakamoto T., Gehrels N., Palmer D. M., Barthelmy S. D., Graziani C., Cannizzo J. K., 2014, *ApJ*, **783**, 24
- Masci F. J., et al., 2019, *PASP*, **131**, 018003
- Matsumoto T., Piran T., Krolik J. H., 2022, *MNRAS*, **511**, 5085
- Mészáros P., Waxman E., 2001, *Phys. Rev. Lett.*, 87, 171102
- Mohan P., An T., Zhang Y., Yang J., Yang X., Wang A., 2022, *ApJ*, **927**, 74
- Murase K., 2018, *Phys. Rev. D*, 97, 081301
- Murase K., Thompson T. A., Lacki B. C., Beacom J. F., 2011, *Phys. Rev. D*, **84**, 043003
- Murase K., Franckowiak A., Maeda K., Margutti R., Beacom J. F., 2019, *ApJ*, **874**, 80
- Nordin J., Brinnel V., Giomi M., Santen J. V., Gal-Yam A., Yaron O., Schulze S., 2019, Transient Name Server Discovery Report, [2019-1231](#), 1
- Nyholm A., et al., 2020, *A&A*, **637**, A73
- Petropoulou M., Dimitrakoudis S., Padovani P., Mastichiadis A., Resconi E., 2015, *MNRAS*, **448**, 2412
- Reimer A., Boettcher M., Buson S., 2019, *Astrophys. J.*, 881, 46
- Reusch S., et al., 2020, GCN Circular, 27872
- Reusch S., et al., 2021, arXiv e-prints, p. [arXiv:2111.09390](#)
- Rodrigues X., Gao S., Fedynitch A., Palladino A., Winter W., 2019, *Astrophys. J. Lett.*, 874, L29
- Rodrigues X., Garrappa S., Gao S., Paliya V. S., Franckowiak A., Winter W., 2021, *ApJ*, **912**, 54
- Santander M., 2019a, GCN Circular, 24981
- Santander M., 2019b, GCN Circular, 25402
- Santander M., 2019c, GCN Circular, 26620
- Santander M., 2020a, GCN Circular, 27651
- Santander M., 2020b, GCN Circular, 27997
- Santander M., 2020c, GCN Circular, [28575](#)
- Santander M., 2021a, GCN Circular, [29951](#)
- Santander M., 2021b, GCN Circular, [29976](#)
- Santander M., 2021c, GCN Circular, [30026](#)
- Santander M., 2021d, GCN Circular, [30342](#)
- Santander M., 2021e, GCN Circular, [30559](#), 1
- Santander M., 2021f, GCN Circular, [30627](#), 1
- Schlegel E. M., 1990, *MNRAS*, **244**, 269
- Senno N., Murase K., Mészáros P., 2016, *Phys. Rev. D*, 93, 083003
- Shappee B. J., et al., 2014, *ApJ*, **788**, 48
- Stanek K. Z., 2018, Transient Name Server Discovery Report, [2018-828](#), 1
- Stecker F. W., Done C., Salamon M. H., Sommers P., 1991, *Phys. Rev. Lett.*, 66, 2697
- Steeghs D., et al., 2019, GRB Coordinates Network, [25255](#), 1
- Stein R., 2019a, in 36th International Cosmic Ray Conference (ICRC2019). p. 1016 ([arXiv:1908.08547](#))
- Stein R., 2019b, GCN Circular, 25225
- Stein R., 2019c, GCN Circular, 25802
- Stein R., 2019d, GCN Circular, 25913
- Stein R., 2019e, GCN Circular, 26341
- Stein R., 2019f, GCN Circular, 26435
- Stein R., 2020a, GCN Circular, 26655
- Stein R., 2020b, GCN Circular, 26696
- Stein R., 2020c, GCN Circular, 27534
- Stein R., 2020d, GCN Circular, 27865
- Stein R., 2020e, GCN Circular, [28210](#)
- Stein R., Franckowiak A., Kasliwal M. M., Andreoni I., Coughlin M., Singer L. P., Masci F., van Velzen S., 2019, The Astronomer's Telegram, [12974](#)
- Stein R., Necker J., Bradascio F., Garrappa S., 2021a, icecube/flarestack: Titan v2.4.1, Zenodo, doi:[10.5281/zenodo.5497486](#), <https://doi.org/10.5281/zenodo.5497486>
- Stein R., et al., 2021b, *Nature Astron.*, 5, 510
- Stein R., et al., 2022, The ZTF Neutrino Follow-Up Program, in preparation
- Strolger L.-G., et al., 2015, *ApJ*, **813**, 93
- Strotjohann N. L., Kowalski M., Franckowiak A., 2019, *Astron. Astrophys.*, 622, L9
- Taboada I., 2016, GCN Circular, [20119](#)
- Taboada I., 2017, GCN Circular, [22105](#)
- Taboada I., 2018, GCN Circular, 23338
- Taboada I., 2019, GCN Circular, 23918
- Tony J., et al., 2019, Transient Name Server Discovery Report, [2019-844](#), 1
- Winter W., Lunardini C., 2021, *Nature Astronomy*, 5, 472

- Woosley S. E., Bloom J. S., 2006, *Ann. Rev. Astron. Astrophys.*, **44**, 507
Zirakashvili V. N., Ptuskin V. S., 2016, *Astroparticle Physics*, **78**, 28
de Jaeger T., et al., 2022, *MNRAS*, **509**, 3427
van Velzen S., et al., 2021, arXiv e-prints, [p. arXiv:2111.09391](#)

APPENDIX A:

In Figure A we show 5σ detections and upper limits for AT2020rng by ASAS-SN and the Zwicky Transient Facility forced-photometry service.

**APPENDIX B:**

In Table B1, the relevant information for all the transients observed by ASAS-SN in IceCube regions is displayed. The first column gives the transient name, followed (in Column 2) by the epoch of the ASAS-SN discovery. In Column 3, we list the IceCube neutrino alert name while column 4 contains the ASAS-SN discovery time. Finally, in Column 5 we give the difference in days between the ASAS-SN and IceCube epochs and in columns 6 the transient type. Interesting sources as defined in Section 3.2 that were discovered within 500 days before the neutrino are discussed in more detail in Section 3.3 while all other sources are not considered potential neutrino counterparts.

Table B1: The transient sample.

Transient	ASAS-SN detection JD	IceCube alert	Alert epoch JD	$\Delta t = t_{\text{ASASSN}} - t_{\text{IceCube}}$ days	Transient type
SN 2021yrf	2459472.9	IC200911A	2459104.1	369	SN Ia
ASASSN-21qp	2459457.8	IC200530A	2458999.8	458	SN Ia
SN 2021vtl	2459442.0	IC200614A	2459015.0	427	SN Ia
SN 2021vpv	2459439.0	IC210608A	2459373.7	65	SN Ia
ASASSN-21oy	2459431.7	IC200512A	2458981.8	450	CV
SN 2021ucx	2459430.1	IC200614A	2459015.0	415	SN Ia
SN 2021rem	2459405.7	IC200410A	2458950.5	455	SN II
SN 2021rgw	2459399.9	IC200410A	2458950.5	449	SN Ia
AT2021qiz	2459394.5	IC160814A	2457615.4	1779	Unknown
ASASSN-21ld	2459380.1	IC201120A	2459173.9	206	Flare
SN 2021oza	2459373.8	IC200410A	2458950.5	423	SN Ia
SN 2021mim	2459365.8	IC200410A	2458950.5	415	SN Ia
SN 2021mid	2459364.9	IC200410A	2458950.5	414	SN Ia
SN 2021jwl	2459329.9	IC191119A	2458806.5	523	SN Ia
ASASSN-21gk	2459322.9	IC190221A	2458535.9	787	CV
SN 2021ipb	2459316.9	IC200410A	2458950.5	366	SN Ia
SN 2021hem	2459310.8	IC200410A	2458950.5	360	SN Ia
SN 2021ghc	2459307.8	IC190819A	2458715.2	593	SN Ia
SN 2021fqb	2459296.0	IC191119A	2458806.5	489	SN Ia
SN 2021ezt	2459293.0	IC200530A	2458999.8	293	SN IIn
AT2021fnf	2459290.7	IC200410A	2458950.5	340	QSO
ASASSN-21dk	2459286.8	IC200921A	2459114.3	172	CV
SN 2021bnw	2459262.9	IC200109A	2458858.5	404	SLSN-I
AT2021cgr	2459257.5	IC201130A	2459184.3	73	Unknown
ASASSN-21at	2459249.8	IC190712A	2458676.6	573	CV
SN 2020aaxo	2459187.8	IC200523A	2458992.6	195	SN Ia
ASASSN-20pb	2459185.8	IC200425A	2458965.5	220	CV
SN 2020yxd	2459170.8	IC200614A	2459015.0	156	SN Ia
SN 2020yfw	2459168.7	IC210608A	2459373.7	-205	SN Ia
SN 2020unl	2459138.1	IC200425A	2458965.5	173	SN Ia
ASASSN-20my	2459131.6	IC190221A	2458535.9	596	CV
ASASSN-20mb	2459106.8	IC200512A	2458981.8	125	CV
AT2020rng	2459089.9	IC210608A	2459373.7	-284	Unknown
ASASSN-20jl	2459061.5	IC200410A	2458950.5	111	CV
SN 2020oye	2459054.8	IC200410A	2458950.5	104	SN Ia

Transient	ASAS-SN discovery JD	IceCube alert	Alert epoch JD	$\Delta_t = t_{\text{ASASSN}} - t_{\text{IceCube}}$ days	Transient type
AT2020neh	2459024.8	IC200410A	2458950.5	74	TDE
SN 2020lsc	2459011.9	IC200410A	2458950.5	61	SN Ia
SN 2020kpx	2458994.8	IC191119A	2458806.5	188	SN Ia
SN 2020joh	2458985.8	IC200410A	2458950.5	35	SN Ia
ASASSN-20eh	2458964.8	IC200530A	2458999.8	-35	CV
AT2020idu	2458962.9	IC200530A	2458999.8	-37	Unknown
ASASSN-20ea	2458957.7	IC200916A	2459109.4	-152	CV
ASASSN-20dz	2458956.6	IC201120A	2459173.9	-217	CV
ASASSN-20dy	2458955.9	IC201221A	2459205.0	-249	CV
AT2020fh5	2458943.1	IC200410A	2458950.5	-7	SN Ia
SN 2020cli	2458909.9	IC200410A	2458950.5	-41	SN Ia
SN 2020czo	2458904.1	IC200109A	2458858.5	46	SN Ia
AT2020cxg	2458899.7	IC160814A	2457615.4	1284	CV
SN 2020zj	2458876.0	IC200410A	2458950.5	-74	SN Ia
AT2020ajp	2458870.1	IC160731A	2457600.6	1270	Unknown
ASASSN-20aq	2458867.2	IC200921A	2459114.3	-247	SN Ia
SN 2020ds	2458863.6	IC201209A	2459192.9	-329	SN Ia
SN 2019zhs	2458851.1	IC191119A	2458806.5	45	SN Ia
ASASSN-19aeb	2458845.7	IC210608A	2459373.7	-528	SN Ia
ASASSN-19abo	2458810.5	IC190819A	2458715.2	95	SN II
ASASSN-19abe	2458792.5	IC200512A	2458981.8	-189	CV
SN 2019stx	2458786.5	IC191122A	2458810.4	-24	SN Ia
ASASSN-19aae	2458784.6	IC210608A	2459373.7	-589	CV
ASASSN-19wi	2458730.8	IC210608A	2459373.7	-643	CV
AT2019pfq	2458730.8	IC210608A	2459373.7	-643	Unknown
SN 2019oml	2458721.6	IC191231A	2458849.0	-127	SN Ia
ASASSN-19uo	2458719.8	IC200410A	2458950.5	-231	SN Ia
ASASSN-19ua	2458715.5	IC200523A	2458992.6	-277	CV
AT2019lvs	2458697.4	IC210608A	2459373.7	-676	Unknown
SN 2019lrc	2458689.0	IC200523A	2458992.6	-304	SN Ia
SN 2019kze	2458679.8	IC210608A	2459373.7	-694	SN Ia
SN 2019ieh	2458673.8	IC200410A	2458950.5	-277	SN Ic
SN 2019igg	2458666.9	IC200410A	2458950.5	-284	SN Ia
ASASSN-19qg	2458661.2	IC200109A	2458858.5	-197	SN Ia
ASASSN-19px	2458657.8	IC200410A	2458950.5	-293	CV
SN 2019gqa	2458644.9	IC200410A	2458950.5	-306	SN Ia
AT2019fxr	2458634.9	IC200410A	2458950.5	-316	Unknown
AT2019dsg	2458618.9	IC191001A	2458758.3	-139	TDE
SN 2019due	2458601.8	IC200410A	2458950.5	-349	SN Ia
ASASSN-19kw	2458600.9	IC190104A	2458487.9	113	SN Ia
SN 2019crd	2458576.9	IC190704A	2458669.3	-92	SN Ia
SN 2019byw	2458572.6	IC200410A	2458950.5	-378	SN Ia
ASASSN-19hm	2458569.6	IC160814A	2457615.4	954	SN Ia
ASASSN-19dw	2458544.5	IC190704A	2458669.3	-125	SN Ia
ASASSN-19dz	2458545.0	IC200410A	2458950.5	-406	SN Ia
SN 2019aah	2458519.6	IC191119A	2458806.5	-287	SN II
ASASSN-19bx	2458516.0	IC200410A	2458950.5	-434	SN Ia
SN 2019agm	2458516.0	IC200410A	2458950.5	-434	SN Ia
SN 2019pe	2458502.0	IC200410A	2458950.5	-449	SN Ia
SN 2019vv	2458502.0	IC191119A	2458806.5	-305	SN Ia
ASASSN-19an	2458493.0	IC200425A	2458965.5	-472	CV
SN 2018kji	2458484.0	IC200410A	2458950.5	-466	SN Ia
ASASSN-18abn	2458465.6	IC191122A	2458810.4	-345	CV
ASASSN-18abl	2458465.4	IC191231A	2458849.0	-384	Stellar outburst
SN 2018ids	2458450.6	IC191001A	2458758.3	-308	SN Ia
SN 2018hom	2458423.8	IC190619A	2458654.1	-230	SN Ic-BL
SN 2018hhn	2458417.7	IC190619A	2458654.1	-236	SN Ia
SN 2018hcr	2458401.6	IC200523A	2458992.6	-591	SN Ia
ASASSN-18um	2458369.5	IC210608A	2459373.7	-1004	CV
SN 2018fng	2458369.5	IC200410A	2458950.5	-581	SN Ia
AT2018fce	2458365.6	IC200410A	2458950.5	-585	Unknown
ASASSN-18rm	2458339.7	IC210608A	2459373.7	-1034	CV
SN 2018eoe	2458338.8	IC210608A	2459373.7	-1035	SN Ib
SN 2018emi	2458333.3	IC200530A	2458999.8	-667	SN Ia
ASASSN-18qo	2458319.0	IC201120A	2459173.9	-842	CV
AT2018dzy	2458320.9	IC210608A	2459373.7	-1053	SN Ia

Transient	ASAS-SN discovery JD	IceCube alert	Alert epoch JD	$\Delta_t = t_{\text{ASASSN}} - t_{\text{IceCube}}$ days	Transient type
AT2018dyd	2458316.8	IC191001A	2458758.3	-442	SN Ia
SN 2018cyh	2458303.5	IC191119A	2458806.5	-503	SN II
ASASSN-18nr	2458289.0	IC210608A	2459373.7	-1085	SN Ia
ASASSN-18mx	2458286.1	IC190619A	2458654.1	-368	SN II
ASASSN-18mn	2458282.6	IC190104A	2458487.9	-205	SN Ia
AT2018chp	2458282.9	IC200410A	2458950.5	-668	Unknown
SN 2018bwr	2458274.7	IC200410A	2458950.5	-676	SN IIn
ASASSN-18ll	2458271.5	IC191119A	2458806.5	-535	Unknown
ASASSN-18kt	2458258.8	IC210510A	2459344.7	-1086	CV
SN 2018bgg	2458250.8	IC181014A	2458406.0	-155	SN Ia
SN 2018bac	2458241.5	IC190704A	2458669.3	-428	SN Ia
ASASSN-18cr	2458162.9	IC200921A	2459114.3	-951	CV
ASASSN-18bs	2458143.6	IC190629A	2458664.3	-521	CV
SN 2018ie	2458140.8	IC171015A	2458041.6	99	SN Ic
SN 2017ivu	2458110.1	IC200410A	2458950.5	-840	SN II
ASASSN-17ot	2458070.8	IC180908A	2458370.3	-300	Unknown
ASASSN-17ou	2458067.7	IC190619A	2458654.1	-586	CV
ASASSN-17oc	2458059.7	IC210608A	2459373.7	-1314	SN Ia
SN 2017hfw	2458046.7	IC201209A	2459192.9	-1146	SN Ic
ASASSN-17od	2458046.1	IC200615A	2459016.1	-970	CV
ASASSN-17lz	2458008.5	IC200410A	2458950.5	-942	SN Ia
AT2017fwf	2457977.8	IC200410A	2458950.5	-973	Unknown
ASASSN-17jz	2457961.9	IC201221A	2459205.0	-1243	ANT
ASASSN-17jt	2457960.1	IC191001A	2458758.3	-798	Unknown
ASASSN-17ji	2457946.5	IC191001A	2458758.3	-812	CV
ASASSN-17ja	2457935.5	IC200410A	2458950.5	-1015	CV
ASASSN-17ii	2457927.9	IC200410A	2458950.5	-1023	SN Ia
ASASSN-17gr	2457897.9	IC200410A	2458950.5	-1053	Unknown
AT2017edw	2457893.8	IC200109A	2458858.5	-965	Unknown
AT2017dtj	2457891.9	IC191119A	2458806.5	-915	Unknown
ASASSN-17ff	2457863.8	IC200109A	2458858.5	-995	SN Ia
ASASSN-17fh	2457864.0	IC200410A	2458950.5	-1086	CV.
ASASSN-17fd	2457863.0	IC191119A	2458806.5	-944	SN Ia
ASASSN-17fd	2457863.0	IC200410A	2458950.5	-1087	SN Ia
SN 2017cne	2457847.0	IC191119A	2458806.5	-960	SN Ia
ASASSN-17ei	2457844.8	IC181014A	2458406.0	-561	CV
SN 2017ciy	2457840.0	IC200530A	2458999.8	-1160	SN Ia
ASASSN-17eb	2457835.6	IC200410A	2458950.5	-1115	SN Ia
ASASSN-17cr	2457805.1	IC200410A	2458950.5	-1145	SN Ia
SN 2017avl	2457802.8	IC191204A	2458822.4	-1020	SN Ia
AT2017jn	2457782.1	IC200410A	2458950.5	-1168	Unknown
ASASSN-17bd	2457777.1	IC200410A	2458950.5	-1173	SN Ia
ASASSN-17bb	2457777.1	IC191119A	2458806.5	-1029	SN Ia
ASASSN-17ae	2457758.1	IC200410A	2458950.5	-1192	SN Ia
ASASSN-16ps	2457753.7	IC190503A	2458607.2	-854	CV
ASASSN-16oo	2457728.6	IC191122A	2458810.4	-1082	SN Ia
AT2016ipd	2457721.9	IC200614A	2459015.0	-1293	Unknown
SN 2016hvu	2457702.8	IC210608A	2459373.7	-1671	SN II
ASASSN-16ie	2457607.8	IC200410A	2458950.5	-1343	SN Ia
ASASSN-16hz	2457601.8	IC200523A	2458992.6	-1391	SN Ia
ASASSN-16fp	2457536.0	IC210608A	2459373.7	-1838	SN Ic-BL
ASASSN-16ex	2457511.9	IC200530A	2458999.8	-1488	SN Ia
SN 2016brw	2457511.9	IC200530A	2458999.8	-1488	SN II
MASTER OT J152333.04+092125.6	2457489.9	IC200410A	2458950.5	-1461	SN Ia
ASASSN-16eg	2457488.0	IC201221A	2459205.0	-1717	CV
ASASSN-16dp	2457479.0	IC191119A	2458806.5	-1328	SN Ia
ASASSN-16ct	2457454.0	IC191119A	2458806.5	-1353	SN Ia
ASASSN-16cq	2457453.8	IC190712A	2458676.6	-1223	CV
SN 2016afa	2457450.0	IC200410A	2458950.5	-1500	SN II
ASASSN-16bg	2457425.0	IC200921A	2459114.3	-1689	SN Ia
MASTER OT J105908.57+103834.8	2457419.0	IC200109A	2458858.5	-1440	SN Ia
PSNJ01534240+2956107	2457386.8	IC200614A	2459015.0	-1628	SN
ASASSN-15ul	2457380.1	IC191119A	2458806.5	-1426	SN Ia
ASASSN-15tp	2457360.5	IC190712A	2458676.6	-1316	CV
ASASSN-15ti	2457357.9	IC200911A	2459104.1	-1746	SN Ia
PSNJ23002463+0137368	2457247.0	IC200523A	2458992.6	-1746	SN Ib

Transient	ASAS-SN discovery JD	IceCube alert	Alert epoch JD	$\Delta_t = t_{\text{ASASSN}} - t_{\text{IceCube}}$ days	Transient type
ASASSN-15nz	2457242.8	IC200410A	2458950.5	-1708	CV
ASASSN-15nr	2457240.9	IC201021A	2459143.8	-1903	SN Ia
ASASSN-15mu	2457222.0	IC190619A	2458654.1	-1432	CV
ASASSN-15mw	2457220.5	IC160814A	2457615.4	-395	blazar candidate
ASASSN-15js	2457163.8	IC200109A	2458858.5	-1695	SN Ia
ASASSN-15jd	2457156.0	IC200410A	2458950.5	-1795	CV
ASASSN-15fu	2457108.7	IC190922A	2458748.9	-1640	CV
PSNJ15053007+0138024	2457101.1	IC191119A	2458806.5	-1705	SN Ia
ASASSN-15fm	2457096.6	IC210510A	2459344.7	-2248	CV
ASASSN-15dz	2457074.1	IC200410A	2458950.5	-1876	SN Ia
ASASSN-15db	2457069.1	IC200410A	2458950.5	-1881	SN Ia
ASASSN-15dd	2457069.1	IC200410A	2458950.5	-1881	SN Ia
ASASSN-15bk	2457042.1	IC200410A	2458950.5	-1908	SN Ia
ASASSN-15bd	2457040.1	IC200410A	2458950.5	-1910	SN IIb
ASASSN-15av	2457036.9	IC191204A	2458822.4	-1786	CV
PSNJ03281419+3801111	2457018.8	IC200911A	2459104.1	-2085	SN
2014ea	2457013.0	IC190704A	2458669.3	-1656	SN Ia
ASASSN-14im	2456932.0	IC200911A	2459104.1	-2172	CV
ASASSN-14hi	2456916.5	IC191215A	2458833.0	-1916	CV
PYPer	2456910.0	IC200911A	2459104.1	-2194	CV
V589Her	2456904.8	IC200410A	2458950.5	-2046	CV
ASASSN-14fq	2456885.6	IC191204A	2458822.4	-1937	CV
CSS111118:051923+155435	2456884.6	IC190712A	2458676.6	-1792	CV
HYPsc	2456867.0	IC200523A	2458992.6	-2126	CV
V544Her	2456857.9	IC200410A	2458950.5	-2093	CV
ASASSN-14dc	2456833.1	IC200614A	2459015.0	-2182	SN
SDSSJ102637.04+475426.3	2456824.7	IC200806A	2459068.1	-2243	CV
ASASSN-14ax	2456782.0	IC200530A	2458999.8	-2218	SN Ia
ASASSN-14an	2456758.0	IC210811A	2459437.6	-2680	Nova
SDSSJ162520.29+120308.7	2456757.9	IC200410A	2458950.5	-2193	CV
2QZJ130441.7+010330	2456736.8	IC201115A	2459168.6	-2432	CV
ASASSN-13dg	2456567.9	IC200614A	2459015.0	-2447	CV
ASASSN-13cw	2456543.9	IC191001A	2458758.3	-2214	CV
HS0218+3229	2456540.9	IC200614A	2459015.0	-2474	CV
1RXSJ185310.0+594509	2456519.8	IC191215A	2458833.0	-2313	CV
ASASJ224349+0809.5	2456518.9	IC190619A	2458654.1	-2135	CV
ASASSN-13bx	2456511.9	IC200523A	2458992.6	-2481	CV
ASASSN-13bw	2456509.5	IC200410A	2458950.5	-2441	CV
V521Peg	2456507.0	IC210608A	2459373.7	-2867	CV
CSS110921:160824+165240	2456482.8	IC200410A	2458950.5	-2468	CV
ASASSN-13bi	2456482.8	IC191119A	2458806.5	-2324	Flare
WYTri	2456481.1	IC200614A	2459015.0	-2534	CV
QWSer	2456477.8	IC200410A	2458950.5	-2473	CV
V368Peg	2456468.5	IC190619A	2458654.1	-2186	CV
CSS080505:163121+103134	2456468.9	IC200410A	2458950.5	-2482	CV
CSS090911:221232+160140	2456459.9	IC210608A	2459373.7	-2914	CV

This paper has been typeset from a $\text{\TeX}/\text{\LaTeX}$ file prepared by the author.